

AD

(Leave blank)

Award Number: W81XWH-08-1-0323

TITLE: Quantitative In Vivo Imaging of Breast Tumor Extracellular Matrix

PRINCIPAL INVESTIGATOR: Xiaoxing Han

CONTRACTING ORGANIZATION:

University of Rochester

Rochester, NY 14642

REPORT DATE: May 2009

TYPE OF REPORT: Annual Summary

PREPARED FOR: U.S. Army Medical Research and Materiel Command
Fort Detrick, Maryland 21702-5012

DISTRIBUTION STATEMENT: (Check one)

☒ Approved for public release; distribution unlimited

☐ Distribution limited to U.S. Government agencies only;
report contains proprietary information

The views, opinions and/or findings contained in this report are those of the author(s) and should not be construed as an official Department of the Army position, policy or decision unless so designated by other documentation.

REPORT DOCUMENTATION PAGE				Form Approved OMB No. 0704-0188	
Public reporting burden for this collection of information is estimated to average 1 hour per response, including the time for reviewing instructions, searching existing data sources, gathering and maintaining the data needed, and completing and reviewing this collection of information. Send comments regarding this burden estimate or any other aspect of this collection of information, including suggestions for reducing this burden to Department of Defense, Washington Headquarters Services, Directorate for Information Operations and Reports (0704-0188), 1215 Jefferson Davis Highway, Suite 1204, Arlington, VA 22202-4302. Respondents should be aware that notwithstanding any other provision of law, no person shall be subject to any penalty for failing to comply with a collection of information if it does not display a currently valid OMB control number. PLEASE DO NOT RETURN YOUR FORM TO THE ABOVE ADDRESS.					
1. REPORT DATE (DD-MM-YYYY) 31-05-2009		2. REPORT TYPE Annual Summary		3. DATES COVERED (From - To) 1 May 2008- 30 Apr 2009	
4. TITLE AND SUBTITLE Quantitative In Vivo Imaging of Breast Tumor Extracellular Matrix				5a. CONTRACT NUMBER	
				5b. GRANT NUMBER W81XWH-08-1-0323	
				5c. PROGRAM ELEMENT NUMBER	
6. AUTHOR(S) Xiaoxing Han Email: hanxxcn@yahoo.com				5d. PROJECT NUMBER	
				5e. TASK NUMBER	
				5f. WORK UNIT NUMBER	
7. PERFORMING ORGANIZATION NAME(S) AND ADDRESS(ES) University of Rochester Department of Biomedical Engineering 601 Elmwood Avenue Box 639 Rochester, NY 14642				8. PERFORMING ORGANIZATION REPORT NUMBER	
9. SPONSORING / MONITORING AGENCY NAME(S) AND ADDRESS(ES) U.S. Army Medical Research and Materiel Command Fort Detrick, Maryland 21702-5012				10. SPONSOR/MONITOR'S ACRONYM(S)	
				11. SPONSOR/MONITOR'S REPORT NUMBER(S)	
12. DISTRIBUTION / AVAILABILITY STATEMENT Distribution Unlimited					
13. SUPPLEMENTARY NOTES					
14. ABSTRACT SHG intensity combined with the F/B ratio provides unique measures of the local density of ordered collagen, as well as the characteristic length scale of this ordering. In order to fully implement F/B ratio measurements to understand the dynamic ordering of collagen in living tumors, we must be able to measure this property <i>in vivo</i> , in intact tissue, which stops us from using a forwards detector. In this annual report, we described ongoing work developing optical methods to quantify the breast tumor collagen SHG F/B scattering ratio in intact tumors <i>in vivo</i> , i.e. without a forwards detector. In future studies this information will be used to determine how manipulation of gene expression by tumor associated macrophages affects collagen ordering, and to determine if SHG measurement of collagen ordering provides a clinically useful measure of metastatic ability.					
15. SUBJECT TERMS Breast Tumor, Collagen, SHG, F/B ratio, In vivo microscopy					
16. SECURITY CLASSIFICATION OF:			17. LIMITATION OF ABSTRACT UU	18. NUMBER OF PAGES 19	19a. NAME OF RESPONSIBLE PERSON USAMRMC
a. REPORT U	b. ABSTRACT U	c. THIS PAGE U			19b. TELEPHONE NUMBER (include area code)

Table of Contents

	<u>Page</u>
Introduction.....	4
Body.....	5
Key Research Accomplishments.....	18
Reportable Outcomes.....	18
Conclusion.....	18
References.....	19

Introduction

Second Harmonic Generation (SHG) is the nonabsorptive combination of two excitation photons into one emission photon within a non-centrosymmetric medium such as a crystal surface, asymmetrically labeled membrane, or collection of properly ordered fibers [1]. In tumor tissue, SHG is generated by arrays of collagen triple helices aligned end-to-end and in parallel rows as fibrillar collagen [2]. SHG is intrinsically sensitive to molecular order: a region of tissue containing unpolymerized collagen triple helices should produce little SHG, while a typical collagen fibril, containing triple helices aligned end-to-end in multiple parallel rows, produces significant SHG.

The internal ordering of collagen fibers within a tumor is a significant factor in the process of tumor metastasis. In breast tumor experiments in mice, tumor cells prefer to move along fibers that are visible by second harmonic generation [3]. Furthermore, tumor cells that are moving along SHG-producing collagen fibers move significantly faster than those cells that are not [4]. Lastly, treatment of tumors with the hormone relaxin, known to alter metastatic ability, has been shown to alter the collagen ordering, detectable by SHG but not by conventional staining [2]. We therefore believe that the assembly of collagen into ordered fibers, visible with SHG, is an important step in tumor metastasis.

In our past work, which has been recently published, we used the forward-to-backward scattering ratio of SHG to understand the axial extent of ordering in collagen fibers [5]. Specifically, the ratio of the forwards- to backwards-scattered SHG (the “F/B ratio”) in the case of tumor collagen is determined by the diameter of the individual ordered fibrils, which bundle together to make up a collagen fiber, with sensitivity to fibril diameters well below the wavelength of light. For example, using 405 nm SHG, we determined that the fibrils in two types of murine mammary tumors had a typical diameter of ~70 nm; this was subsequently confirmed by transmission electron microscopy (TEM) [5]. The fibril diameter provides important insight into tumor collagen metabolism (i.e. collagen synthesis as well as MMP activity) and these measurements can be thought of as equivalent to performing electron microscopy in intact tissue, without the fixing, sectioning, dehydration, and metal coating (and resultant artifacts) required for TEM.

From this work, we see that SHG intensity, combined with the F/B ratio, provide unique measures of the local density of ordered collagen, as well as of the characteristic length scale of this ordering. In order to fully implement F/B ratio measurements to understand the dynamic ordering of collagen in living tumors, we must be able to measure this property *in vivo*, in intact tissue, which stops us from using a forwards detector. Therefore, in this annual report, we will describe ongoing work developing optical methods to quantify the F/B scattering ratio in intact tumors *in vivo*, i.e. without a forwards detector. These methods will allow future biological

studies of the cellular and molecular mechanisms by which the ordering of tumor collagen is governed. Specifically, in future studies this information will be used to determine how manipulation of gene expression by tumor associated macrophages affects collagen ordering, and to determine if SHG measurement of collagen ordering provides a clinically useful measure of metastatic ability

Body

We are now concluding the first year of this grant, here in the Department of Biomedical Engineering at the University of Rochester Medical Center.

Theory

For Second Harmonic Generation, the SHG dipole $\vec{P}_{2\nu}$ can be treated as a new SHG source induced by the excitation E field, \vec{E}_ν .

$$\begin{aligned}\vec{S}_{2\nu} &= \vec{\chi}^{(2)}(-2\nu; \nu, \nu) : \vec{E}_\nu \vec{E}_\nu \\ \vec{S}_{2\nu}(\vec{r}_0) &= \vec{\chi}^{(2)}(\vec{r}_0) : \vec{E}_\nu(\vec{r}_0) \vec{E}_\nu(\vec{r}_0)\end{aligned}\quad (1)$$

For simplicity, we assume $\vec{S}_{2\nu}(\vec{r}_0)$ is polarized in the same direction as $\vec{E}_\nu(\vec{r}_0)$, then the tensor equation can be simplified to a scalar equation:

$$S_{2\nu}(\vec{r}_0) = \chi^{(2)}(\vec{r}_0) E_\nu^2(\vec{r}_0) \quad (2)$$

The propagation of the SHG field emitted from this SHG source in free space can be described by a Helmholtz equation

$$(\nabla^2 + 4\pi^2 k_{2\nu}^2) E_{2\nu}(\vec{r}) = -S_{2\nu}(\vec{r}) \quad (3) \quad \text{where, } k_{2\nu} = n \frac{2\nu}{c}$$

If we consider only far-field scattering, the Fraunhofer approximation can be applied:

$$E_{2\nu}(\vec{r}) = \frac{1}{4\pi r} e^{i2\pi k r} \int e^{-i2\pi k \hat{r} \cdot \vec{r}_0} S_{2\nu}(\vec{r}_0) d^3 \vec{r}_0 \quad (4)$$

For the excitation beam E field in the objective focal point, we use a 3-D-Gaussian approximation

$$E_\nu(\vec{r}_0) = E_\nu e^{-\frac{\rho_0^2}{\omega_0^2} - \frac{z_0^2}{\omega_z^2} + i2\pi(k_\nu - \delta k_\nu)z_0} \quad (5)$$

Where ω_0 and ω_z are the field waist in the lateral and axial directions, respectively.

δk_ν represents the π Gouy phase shift in the vicinity of the Gaussian beam focal spot.

$$\delta k_v = \frac{1}{\pi \omega_0^2 k_v} \quad \omega_0 = \frac{0.32 \lambda_v}{n_v \sin \Theta} \quad \omega_z = \frac{0.53 \lambda_v}{n_v (1 - \cos \Theta)}$$

$n_v \sin \Theta$ is the numeric aperture(N.A.) of the objective.

Substitute $E_v(\vec{r}_0)$ in equation (2) with equation (5), and replace $S_{2v}(\vec{r}_0)$ in equation (4) with equation (2).

$$E_{2v}(\vec{r}) = \frac{1}{4\pi r} e^{i2\pi k_{2v} r} \chi^{(2)} E_v^2 \iiint_{\text{fiber}} e^{-i2\pi \frac{k_{2v}}{r} (xx_0 + yy_0 + zz_0)} e^{-2\frac{(x_0^2 + y_0^2)}{\omega_0^2} - 2\frac{z_0^2}{\omega_z^2} + i4\pi(k_v - \delta k_v)z_0} dx_0 dy_0 dz_0$$

$$\sim \int_{-\infty}^{+\infty} dx_0 \int_{-R_0}^{+R_0} dy_0 \int_{-\sqrt{R_0^2 - y_0^2}}^{\sqrt{R_0^2 - y_0^2}} dz_0 e^{-i2\pi \frac{k_{2v}}{r} (xx_0 + yy_0 + zz_0)} e^{-2\frac{(x_0^2 + y_0^2)}{\omega_0^2} - 2\frac{z_0^2}{\omega_z^2} + i4\pi(k_v - \delta k_v)z_0} \quad (6)$$

where $x = r \sin \theta \cos \varphi$, $y = r \sin \theta \sin \varphi$, $z = r \cos \theta$, R_0 is the radius of the collagen fiber.

The SHG intensity spatial distribution is then a function of R_0 , θ and φ .

$$I_{2v}(\vec{r}) = (1 - \sin^2 \theta \cos^2 \varphi) |E_{2v}(\vec{r})|^2 \quad (7)$$

The ratio of forward to backward propagating SHG intensity can then be expressed as a function of tumor collagen fiber radius:

$$\frac{F}{B}(R_0) = \frac{\int_0^{\pi/2} \int_0^{2\pi} (1 - \sin^2 \theta \cos^2 \varphi) |E_{2v}(R_0, \theta, \varphi)|^2 d\varphi d\theta}{\int_{\pi/2}^{\pi} \int_0^{2\pi} (1 - \sin^2 \theta \cos^2 \varphi) |E_{2v}(R_0, \theta, \varphi)|^2 d\varphi d\theta} \quad (8)$$

The result of this calculation is shown in the B/F ratio vs. collagen fiber diameter plot below. [1]

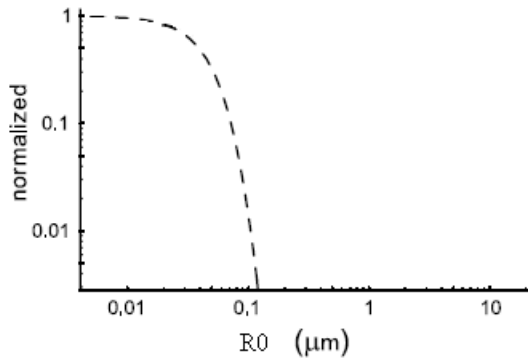


Fig. 1 B/F ratio vs. collagen fiber diameter

Optical Setup

The optical setup we are using to measure the SHG F/B ratio of tumor collagen *in vivo*, in the backward channel only, is shown in figure 2 below. The SHG signal was

generated by a Spectra Physics MaiTai Ti:Sapphire laser, providing 100fs pulses at 80 MHz and 810 nm . The beam was then steered and generated a 700um x 700um scanning area on the sample plane. The scanning system was connected to an Olympus BX61W upright microscope. The focusing objective is an Olympus UMPLFL20XW water immersion lenses (20× , 0.5 N.A.). The objective was used to focus the excitation beam on the sample and at the same time collect the backscattered SHG signal. The backscattered SHG signal was collected by the objective, converged by the tube lens, and collimated by the pupil lens. The collimated SHG beam was then de-scanned and focused again on the pinhole plane by the collector lens. The focal lengths of the pupil lens and the collector lens are 54mm and 185mm respectively, and size of the pinholes on the variable pinhole turret are 60um , 100um, 150um , 200um and 7000um . The SHG beam was separated from the excitation beam by a dichroic mirror (Chroma 670 DCSX) and a band pass filter centered at 405 nm (Chroma HQ405/30m -2P) placed after the pinhole, and was detected by a photomultiplier tube (HC125-02, Hamamatsu).

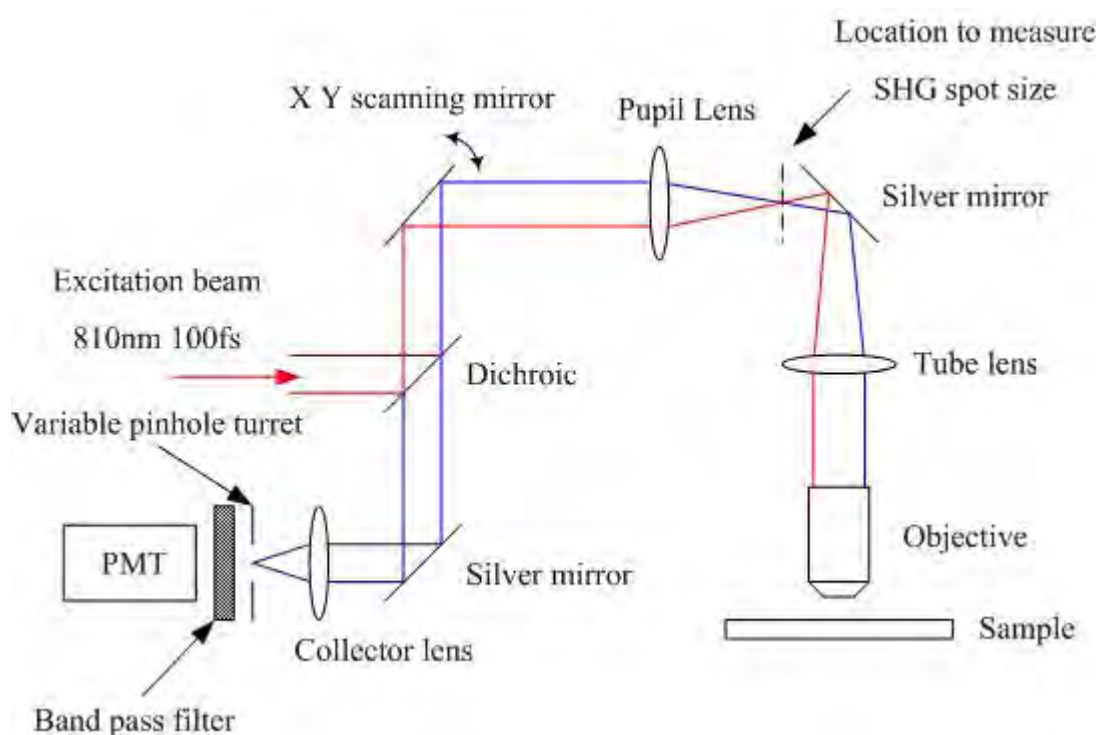


Fig.2. Experimental setup for *in vivo* measurement of tumor collagen SHG F/B ratio

To measure tumor collagen SHG F/B ratio *in vivo* with only the backward channel, we will generate a series of images of the SHG from the tumor surface through a series of confocal pinholes of different sizes. The resultant signal-versus-pinhole-size curve for identified fibers or regions can then be analyzed to produce a number that is proportional to the true F/B ratio. The constant of proportionality is a function of the scattering properties of the underlying tissue. To determine that constant of proportionality we will sprinkle beads on the sample that emit fluorescence at the same wavelength as our SHG with a known F/B ratio, and measure their apparent F/B ratio. The true F/B ratio of the collagen fibers can then be extrapolated.

Determining backward propagating SHG spot size on the pinhole plane

To accomplish this measurement, the first thing we need to do is determine the size of the confocal pinholes, relative to the SHG intensity distribution, by measuring the spot size of only the backward propagating SHG in the confocal plane. Since we are measuring the pinhole plane spot size of only the backward propagating SHG, we need to avoid any backscattering of the forward propagating SHG. An MDA-MB-361 tumor sample was sectioned fresh frozen into 10 μ m thin slices, spread out on a coverslip and dried overnight in a refrigerator for good adhesion between the sample sections and coverslip. The coverslip was then flipped over, with the sample side facing down, submerged in PBS, and with the excitation beam transmitting through the coverslip. The sample was submerged in saline here to minimize the refractive index change and, thus, reduce the back reflection of the forward propagating SHG. The saline container is a cup with a 4cm diameter and 4 cm depth. It was painted black to absorb forward propagating SHG that goes through the sample section.

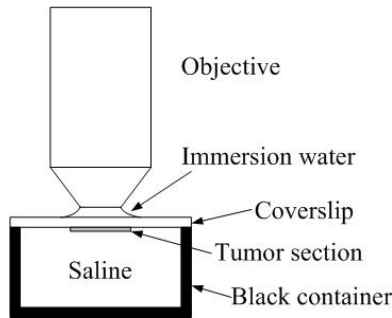


Fig. 3 Configuration of objective, sample, and scatterer holder

To determine the SHG spot size on the pinhole plane, we measured the SHG spot size directly with a CCD camera (SPOT RT3, SciTech) at the location depicted in figure 2. The real SHG spot on the pinhole plane is just a magnified version of the spot we captured with the CCD camera. The magnification factor is the ratio of the focal length of the pupil lens and collection lens.

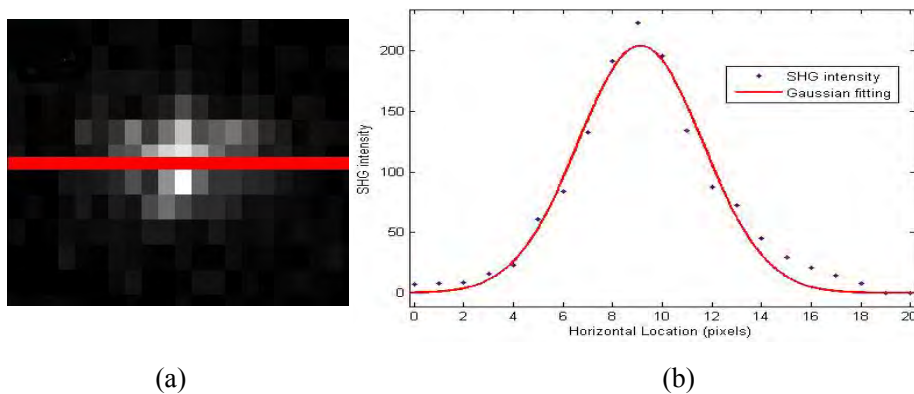


Fig. 4 Determination of SHG spot size. (a) CCD captured image of SHG focal spot after the tube lens (b) SHG intensity along the straight line that goes through the center of SHG spot. The red straight line in (a) is the line along which SHG intensities are measured. The red curve in (b) is the Gaussian fit to the intensities we measured in (a)

As shown in the figure 4 above, we drew a straight line through the center of the SHG spot captured by CCD camera, and measured the SHG intensity along this line. The SHG intensity vs. horizontal location data set was then plotted in figure 4b as a series of separate points, and fitted to a Gaussian Model, $y = a \exp[-(\frac{x-b}{c})^2]$. When the SHG intensity decays from its maxima to $1/e^2$ of its maxima, the width between those two pixels with the same SHG intensity, i.e. $2\sqrt{2}c$, was taken as the SHG spot size. This measurement was repeated 20 times in 20 different regions of interest, evenly spread over the entire sample. The average spot size is 9.34 pixels or 69 μm . Taking into account the magnification factor of the pupil and collector lens, the average pinhole plane spot size of only the backward propagating SHG is 236.8 μm . We already knew that the diameters of the five pinholes on the pinhole turret are 60 μm 100 μm 150 μm 200 μm to 7000 μm respectively. That is 0.24ω , 0.4ω , 0.6ω , 0.8ω and 28ω , where ω stands for the pinhole plane SHG spot size.

Measurement of SHG intensity varied with pinhole size

Before doing *in vivo* measurements of collagen SHG F/B ratio on full size tumors, we tested our idea on an easier and more reproducible model by changing the saline in the black container to whole milk. Milk is an efficient scatterer, with its optical properties well studied in the literature. For whole milk, the value of the absorption coefficient is $\mu_a = 0.7\text{cm}^{-1}$, the reduced scattering coefficient is $\mu_s' = 45\text{cm}^{-1}$ at 405nm, the anisotropic factor is $g = 0.7$, and the absorption coefficient is $\mu_s = 150\text{cm}^{-1}$ [6]. We then measured collagen SHG versus pinhole size in thin sections on top of whole milk, where the backscattering of the forward propagating SHG in the whole milk mimicked the back scattering in a full size tumor.

To get the real value of the tumor collagen SHG F/B ratio, we applied a dilute solution of 10 μm diameter blue fluorescent polystyrene beads (10m 365415, Invitrogen) to the surface of our sample. The real collagen SHG F/B ratio can be calculated by comparing the measured F/B ratio of in-focus calibration beads to the ratio measured on the same day in beads in saline between two coverslips

$$\frac{\text{measured collagen SHG F / B Ratio}}{\text{measured beads TPEF F / B Ratio}} = \frac{\text{real collagen SHG F / B Ratio}}{\text{real beads TPEF F / B Ratio}}$$

We prepared 5 thin tumor sections from one full tumor sample. For each slice we took 5 back detected SHG images with the pinhole size varied from 60 μm 100 μm 150 μm 200 μm to 7000 μm . One of these image sets is shown below.

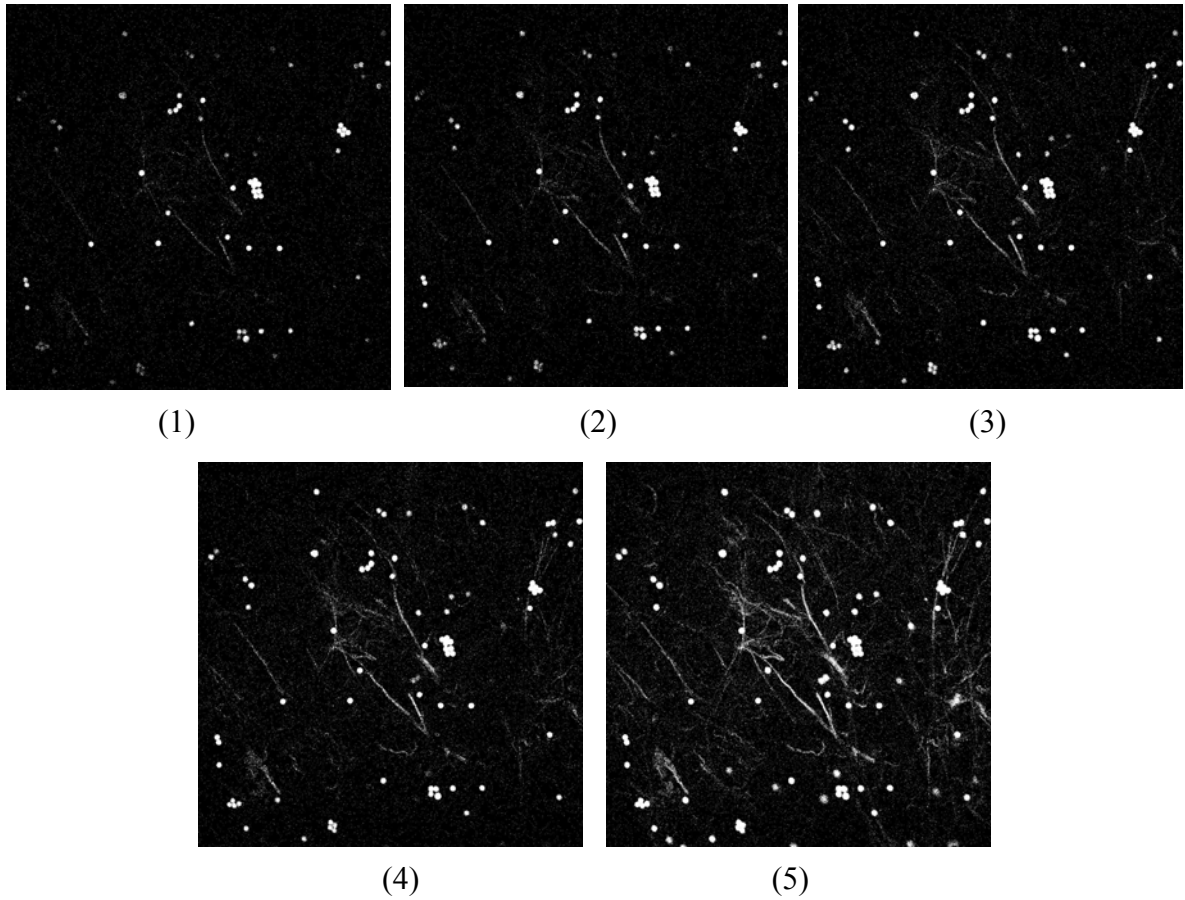


Fig. 5 SHG images of a tumor thin section on top of whole milk. Images 1-5 are SHG images of the same tumor thin section when the size of the pinhole varied from 60 μ m, 100 μ m, 150 μ m, 200 μ m, to 7000 μ m. The bright spots are calibration blue fluorescent polystyrene beads.

The bright spots in these images are calibration blue fluorescent polystyrene beads. In each set of images, from one slice, we picked 3 small regions of interest around collagen fibers and 5 regions of interest around the calibration beads. SHG intensities in these collagen and bead ROIs were measured using ImageJ and normalized so that the maximum SHG intensity measured with the largest pinhole was set to 1. The average SHG intensity of all 15 collagen ROIs and the average intensity of all 25 bead ROIs vs. pinhole size plot is shown below.

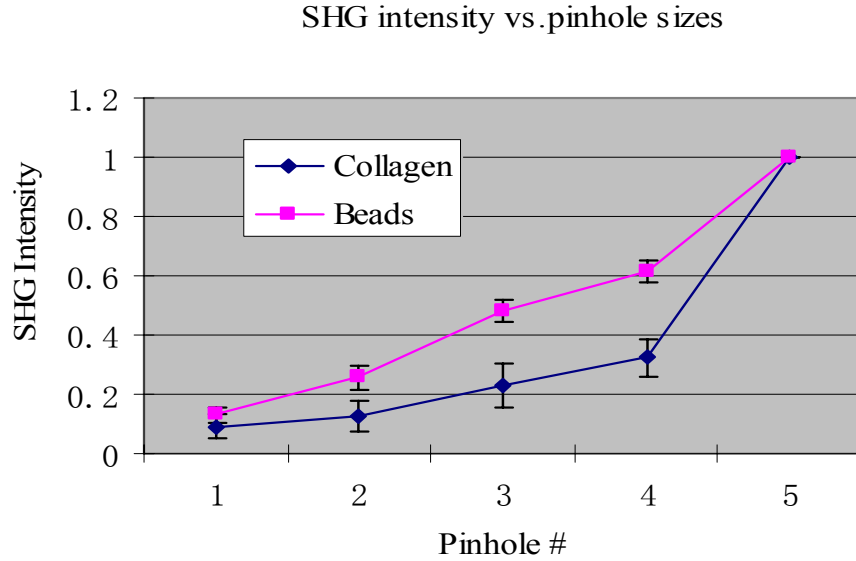


Fig. 6 Average SHG intensity of all 15 collagen ROIs and average SHG intensity of all 25 bead ROIs at different pinhole sizes. The error bars are standard deviation. Note the horizontal axis is highly nonlinear (pinhole #5 is far larger than #4).

Each point in Figure 6 above is equivalent to the integral from $-r$ to r of the intensity distribution of back-scattered plus forward-scattered-and-subsequently-back-scattered light in the confocal plane, where r is the radius of the pinhole. The separation between the collagen curve and the bead curve implies different F/B ratios of these two samples. In order to accurately model this data and extract an F/B ratio, we need to find a good model for the functional form of the radial intensity distribution, at the confocal plane, of the forward-scattered SHG that is subsequently back-scattered.

Angular Distribution of Forward Propagating SHG from tumor collagen

Angular distribution of forward propagating SHG from tumor collagen can be measured by imaging the Fourier plane of the imaging objectives. As shown below, light beams coming in from different directions will be focused to different spots on the Fourier plane of the imaging lens.

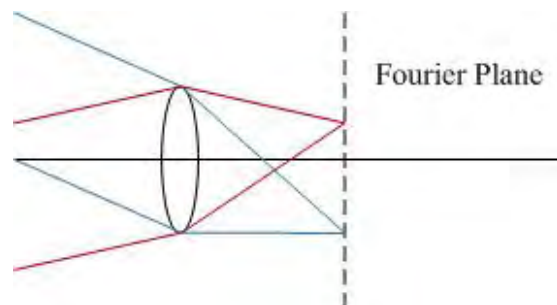


Fig 7. Fourier plane of imaging objective

An image of the Fourier plane of the imaging objective would be a map for the incoming signal beam angular distribution.

As a calibration step, we imaged the Fourier plane of the objective when the sample is a solution of the Cascade Blue fluorescent dye.

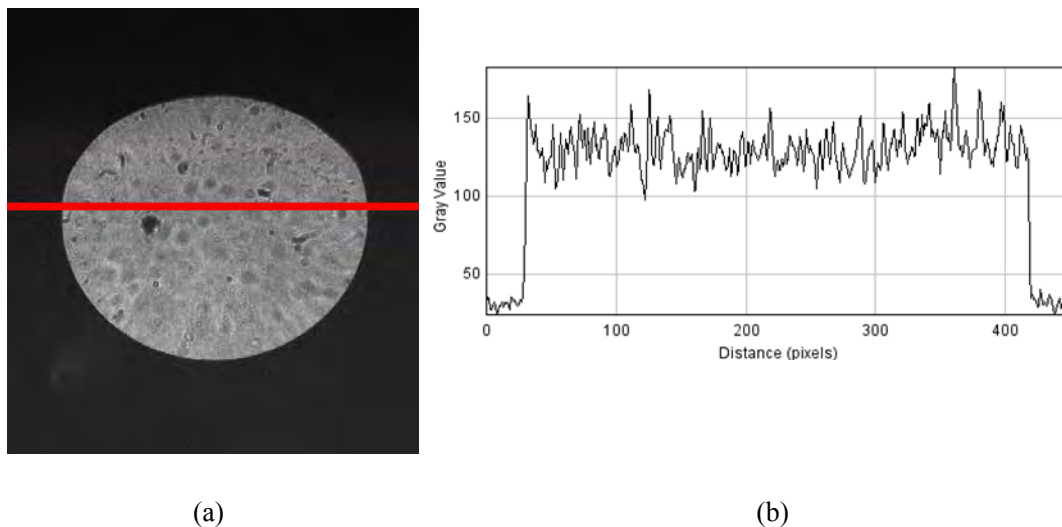


Fig 8. (a) Image of Fourier plane when the sample is a solution of cascade blue fluorescent dye
(b) Intensity distribution along the red line in(a)

As expected, the Fourier plane is a uniform bright field, since fluorescent dyes emit uniformly at all directions. We then drew a straight line across the center of the pattern, and plotted the signal intensity along this line. The NA of the objective is 0.5, which gives us the maximum collection angle of the objective: 45 degrees. The bright field in the Fourier plane image is 400 pixels across, which means every pixel in this image represents 0.11 degrees of collection angle.

We then switched the sample to a thin tumor section, and scanned over a small region of interest. The average Fourier plane image is shown below

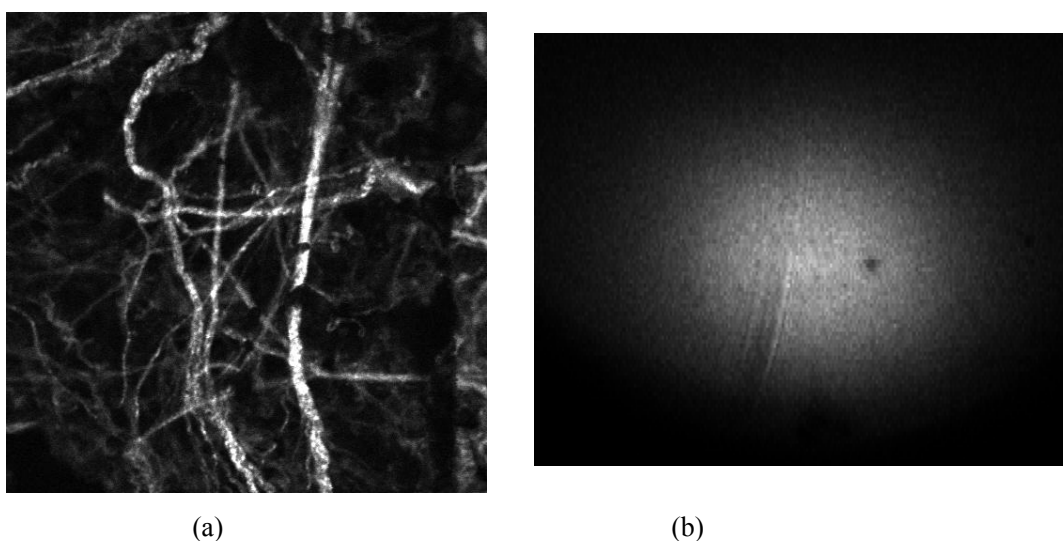


Fig 9 (a) region of interest we picked in the tumor collagen sample
(b) Average image of fourier plane

Again, we drew a straight line across the center of the Fourier plane image, and plotted the signal intensity along the line.

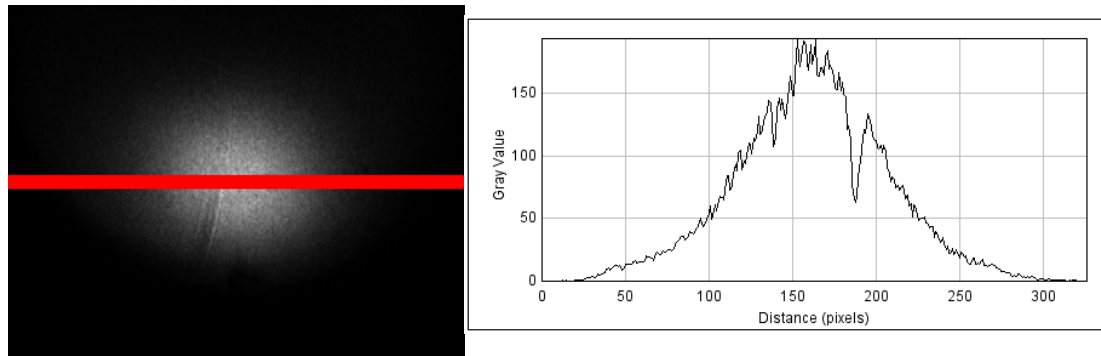


Fig 10 (a) Average image of fourier plane. The sample is tumor collagen in ROI.
(b) Intensity distribution along the red line in (a)

Since one pixel in this image represents a collection angle of 0.11 degrees, we can then plot this angular distribution of forward propagating SHG from tumor collagen in radial coordinates, where the light source is located at the center and the right half of the plane represents the forward direction.

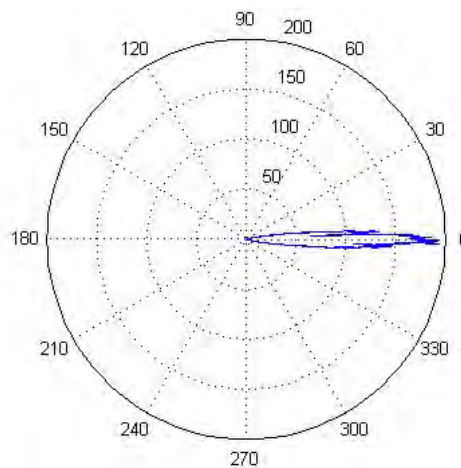


Fig 11 Angular intensity distribution of forward propagating SHG from tumor collagen

Monte Carlo simulation

To find an accurate model for the radial intensity distribution of the back scattered forward propagating SHG, we need to run a Monte Carlo simulation to simulate SHG light propagation in tumor tissue. Except for the angular distribution of the forward propagating SHG from tumor collagen, we also need to know some optical properties of tumor tissue as inputs to the Monte Carlo simulation. We looked through the literature on tumor imaging, and quoted from other investigators' work, the basic optical parameters of breast tumor tissue. The overall refractive index of breast tumor is 1.42 and the optical density is 0.2 in 405nm, according to H Key et al [7], while the average refractive index of a single tumor cell is 1.38 at 405nm, according to Björn Kemper et al [8]. We also imaged a stained thin section of 4T1 tumor to measure the average size of tumor cells and estimate the number density of tumor cells in breast tumor tissue. The average size of tumor cells was found to be $10\text{ }\mu\text{m}$ and the number density of tumor cells in breast tumor tissue is 1 million cells/ mm^3 .

The Monte Carlo simulation was done with a commonly used optical design and simulation tool LightTools(Optical Research Associate, Pasadena, California).

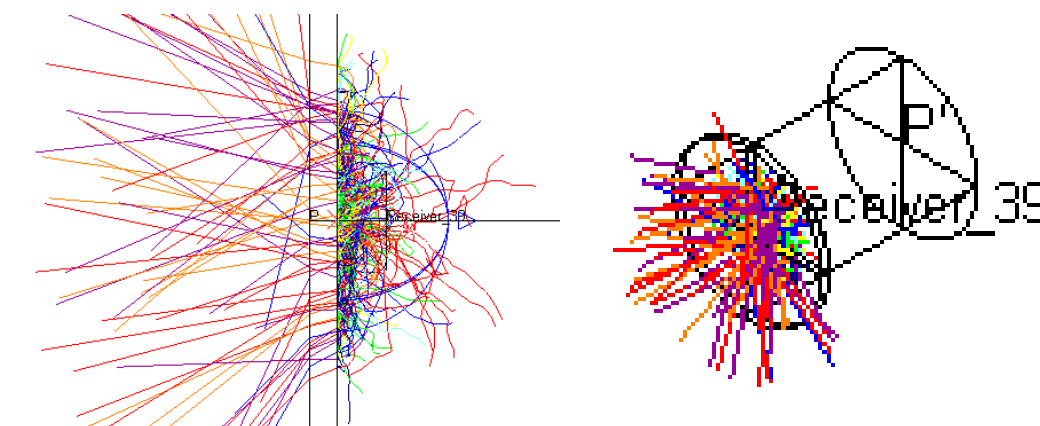


Fig 12. Monte Carlo simulation of light propagation in tumor tissue.

The infinitely long tube represents the tumor; the thin plate represents the detector with its front surface put right on the “tumor” top surface

In this simulation, the shape of the tumor is simplified to be an infinitely long tube with an infinitely wide outer diameter, so that no light escapes from side and bottom surfaces. The thin plate is the detector, with its front surface put right on the “tumor” top surface to measure the back scattered forward propagating SHG. The optical properties of the “tumor” are defined by values from literature and measurement. We used two different sources in the simulation to simulate TPEF from fluorescent beads and SHG from tumor collagen.

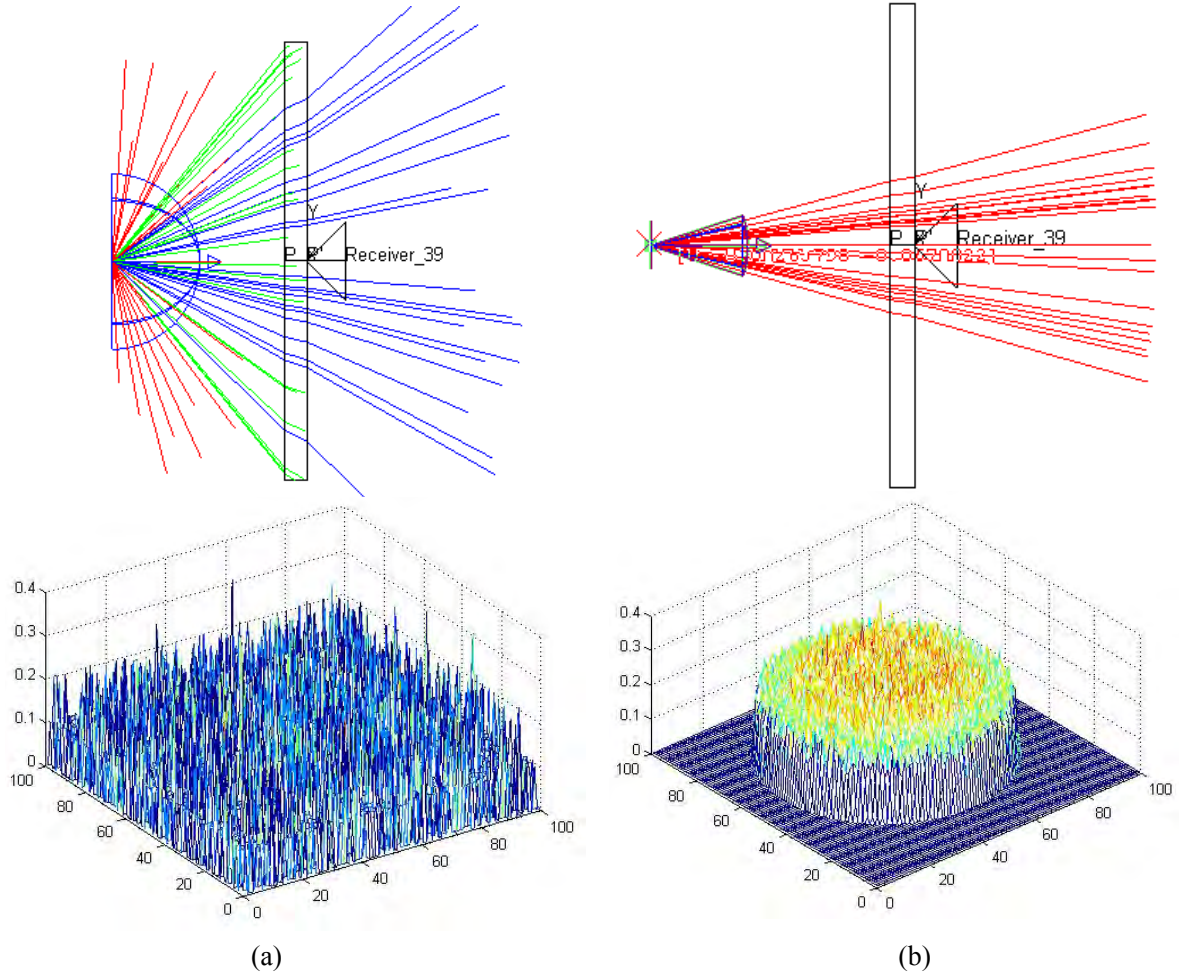


Fig 13 Light source used in Monte Carlo simulation

- (a) TPEF from fluorescent beads is uniform at all directions
- (b) SHG from tumor collagen forms a narrow beam.

The TPEF signal from fluorescent beads emits uniformly to all directions, while the forward propagating SHG forms a narrow beam with defined angular distribution. By putting the detector in front of the light source, we can simulate the beam profile of these two different sources, as shown in the figure(13) above.

The radial intensity distribution of the back scattered forward propagating TPEF or SHG, generated by Monte Carlo simulation, is shown below.

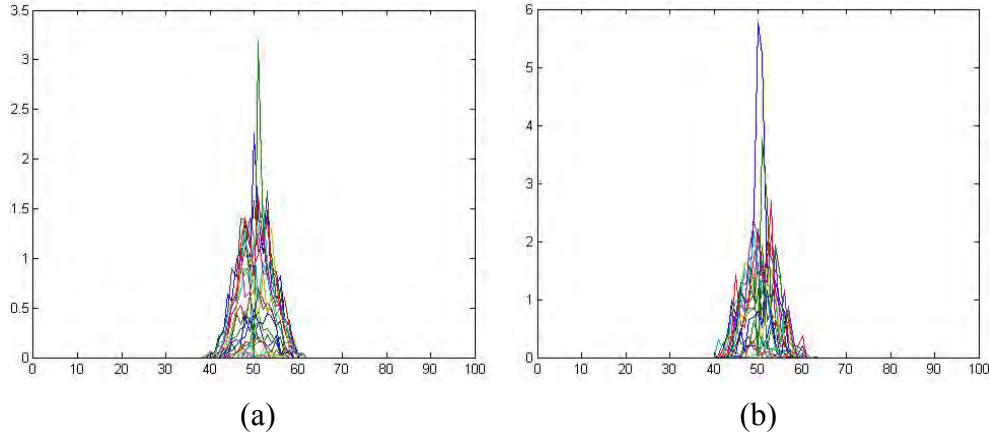


Fig 14 Intensity distribution of the back scattered forward propagating signal generated by Monte Carlo simulation (a) TPEF from fluorescent beads (b) SHG from tumor collagen

Intensity plots of different colors represent cross sections parallel to the y axis, while the x location is increased by 0.01 inch increments. Putting them together in the same plot gives us the overall intensity profile. It is interesting to find out that the intensity distribution of the back scattered TPEF and SHG are so similar, although the angular distribution of the TPEF from fluorescent beads is so different from the angular distribution of the SHG from tumor collagen.

Fitting model

We tried to fit the intensity distribution of the back scattered forward propagating TPEF or SHG to several functional forms and found out that a simple exponential decay fit the simulation results best. The radial intensity distribution of the back scattered forward propagating TPEF and SHG can be expressed as

$$C(r) = C_0 \exp(-r / 3.5485)$$

$$B(r) = B_0 \exp(-r / 3.5137)$$

Where $B(r)$ and $C(r)$ represent backscattered TPEF from beads and backscattered SHG from tumor collagen, respectively. B_0 and C_0 are maximum intensities of the back scattered signals. Note that the unit of radial distance in these equations is 0.01 inches or 254 μm .

The direct backward propagating SHG or TPEF has a Gaussian intensity profile,

$$A(r) = A_0 \exp[-(r / \omega_r)^2]$$

where ω_r can be estimated by

$$\omega_r = \frac{0.32\lambda}{\sqrt{2}NA} = \frac{0.32 \times 810}{1.414 \times 0.5} = 366.5642nm$$

By comparing the characteristic length of the direct backward propagating signal and the backscattered forward propagating signal

$$\frac{3.5485 \times 254um}{366.5642nm} = 2458.83$$

we can then come up with a model to fit to the back detected total signal intensity data, which is normalized to the maximum intensity with the largest pinhole size.

$$I(r) = \frac{\int_{-r}^r \left\{ \exp(-r^2) + \left(\frac{F}{B} \right) C e^{-\frac{|r|}{2458.83}} \right\} dr}{\int_{-28}^{28} \left\{ \exp(-r^2) + \left(\frac{F}{B} \right) C e^{-\frac{|r|}{2458.83}} \right\} dr} \quad (9)$$

Constant parameter C represents the fraction of the forward propagating SHG that finally got back scattered by the tumor or tissue. Normalized back detected SHG or TPEF intensity vs. pinhole size curves are shown below (C=0.1).

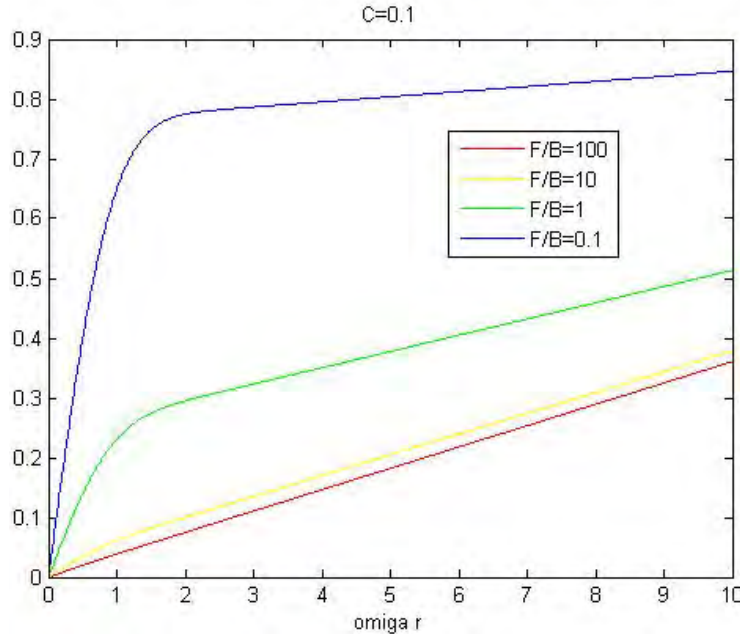


Fig 15. Normalized back detected total signal vs. pinhole size.
Different curves represent samples with different F/B ratios

Along the horizontal axis is plotted pinhole size in units of ω_r , and different curves represent samples with different F/B ratios. By fitting the back detected SHG or TPEF intensity vs. pinhole size data to this model, we can generate $\left(\frac{F}{B} \right) C$ values for both

fluorescent beads and tumor collagen. We can then calculate the real $\left(\frac{F}{B} \right)$ ratio of

tumor collagen by $\frac{\left(\frac{F}{B}\right)_{collagen}}{\left(\frac{F}{B}\right)_{collagen} C} = \frac{\left(\frac{F}{B}\right)_{beads}}{\left(\frac{F}{B}\right)_{beads} C}$, since we already know the real

$\left(\frac{F}{B}\right)$ ratio of fluorescent beads.

We noticed from this plot that by cleverly choosing the size of the pinhole, we can maximize the separation between different curves, and thus, get a more accurate $\frac{F}{B}$ ratio value of the sample. We also noticed that the separation between the $\frac{F}{B} = 0.1$ curve and the $\frac{F}{B} = 1$ curve is much larger than the separation between the $\frac{F}{B} = 10$ curve and the $\frac{F}{B} = 100$ curve. This implies that this method is only good for samples with a low $\left(\frac{F}{B}\right)$ ratio.

Key Research Accomplishments in the Past Year

- 1) We have built up the confocal SHG system to measure the tumor collagen SHG F/B ratio in the backward direction.
- 2) We have imaged the Fourier plane of the imaging objective when the sample is tumor collagen.
- 3) We have measured the angular intensity distribution of forward propagating SHG from tumor collagen.
- 4) We have simulated forward propagating SHG light propagation in tumor tissue with a Monte Carlo simulation.
- 5) We have found a good model to fit to the back detected total TPEF or SHG signal vs. pinhole size data.

Reportable outcomes

During the past year, I presented a contributed poster at the Optical Society of America annual meeting

X. Han et al, "Assessment of Second Harmonic Properties of Tumor Collagen," in Frontiers in Optics, October 19, 2008, Rochester, NY, Joint FIO/LS Poster Session I (JSuA) paper JSuA14.

Conclusion

In the past year, we have built up the experimental set up. We have proved

theoretically the possibility of predicting tumor collagen fibril diameter by measuring the SHG F/B ratio. We have experimentally measured tumor collagen SHG angular distribution. And we have simulated SHG light propagation in tumor tissue with a Monte Carlo simulation. Overall we have finished the experiment design and our next step will be to carry out these experiments with real tumor tissue samples, to test the validity of this method. These facts suggest that we are making significant progress, progress that has been enabled by the generous support of the BCRP Predoc Traineeship Award.

References

- [1] Mertz, J. and L. Moreaux (2001) . "Second-harmonic generation by focused excitation of inhomogeneously distributed scatterers." *Opt. Commun.* **196**(1-6): 325-330.
- [2] Brown, E., T. McKee, et al. (2003) . "Dynamic imaging of collagen and its modulation in tumors in vivo using second-harmonic generation." *Nat Med* **9**(6): 796-800.
- [3] Sidani, M., J. Wyckoff, et al. (2006). "Probing the microenvironment of mammary tumors using multiphoton microscopy." *J Mammary Gland Biol Neoplasia* **11**(2): 151-63.
- [4] Wang, W., J. B. Wyckoff, et al. (2002). "Single cell behavior in metastatic primary mammary tumors correlated with gene expression patterns revealed by molecular profiling." *Cancer Res* **62**(21): 6278-88.
- [5] Han, X., R. M. Burke, et al. (2008). "Second harmonic properties of tumor collagen: determining the structural relationship between reactive stroma and healthy stroma." *Optics Express* **16**(3): 1846-1859.
- [6] Jianwei Qin, et al., "Measurement of the absorption and scattering properties of turbid liquid foods using hyperspectral imaging," *Applied Spectroscopy* 61, 388-396 (2007)
- [7] H Key et al, "Monte Carlo modelling of light propagation in breast tissue" *Phys. Med. Biol.*, 1991, vol.36, No 5, 591-602.
- [8] Björn Kemper et al., "Integral refractive index determination of living suspension cells by multifocus digital holographic phase contrast microscopy," *Journal of Biomedical Optics* 12(5), Sept. 2007 054009.